# Chapter 5

# Shock Interaction with a Right-Angled Wedge: Diffraction and Reflection in an Extended Chaplygin Gas

## 5.1 Introduction

There is much interest in predicting the nature of waves when a weak shock hits the wedge corner. The reflection-diffraction phenomenon occurs due to the impact when a weak shock is incident on the wedge, particularly near the corner of the wedge.

Much work has been carried out on characterizing the regular and Mach reflection configurations when the incident shock reflects off the wedge in gas dynamics [2, 66–69, 71, 134]. Most studies that have been carried out in [72, 73, 78–80, 135, 136] deal with the reflection-diffraction phenomenon in an ideal gas. The significant studies

done to show real gas effects on the reflection-diffraction phenomenon are presented in [76, 77, 81, 83].

The linear solution for the shock reflection-diffraction problem in isentropic gas was presented in [72], and later, the solution was modified using nonlinear geometric acoustic theory in [73]. The study presented in this chapter is influenced by the work done in [72, 73, 83, 137]. This chapter considers the mathematical problem of shock hitting the right-angle wedge [73].

This chapter is arranged in the following sections. In Section 5.2, fundamental equations of gas dynamics explaining the reflection-diffraction phenomenon in extended Chaplygin gas, along with boundary conditions, are presented. To find the asymptotic expressions of variables in states $(\overline{1})$ and $(\overline{2})$, the Rankine-Hugoniot (R-H) conditions are elaborated in Section 5.3, and the asymptotic expressions for state variables are obtained. The behaviour of the asymptotic expansions in the diffracted region is presented in Section 5.4. Near the boundary of the diffracted region, a singularity is found, and in Section 5.5, the nonlinear expansion of solutions is illustrated near the singularity. The results for two special cases, (i) when the shock comes off a wedge and (ii) when the shock hits a thin screen, are described in Section 5.6. The behaviour of nonlinear expansions near a singular point is discussed in Section 5.7. The results and various graphs are plotted in Section 5.8. In Section 5.9, the conclusions of the overall study are elaborated.

## 5.2 Fundamental equations and Configuration of shock reflection-diffraction in self-similar flow

In this section, Euler equations in extended Chaplygin gas are considered with appropriate boundary conditions describing the reflection-diffraction phenomenon by a right-angled wedge. By introducing self-similar variables, the governing equations are presented in a self-similar flow. The regions for reflected and diffracted wavefronts in the self-similar planes are given.

The two-dimensional Euler equations [71] in gas dynamics are given by

$$\begin{aligned} &\rho_t + (\rho U)_X + (\rho V)_Y = 0, \\ &(\rho U)_t + (\rho U^2 + p)_X + (\rho UV)_Y = 0, \\ &(\rho V)_t + (\rho UV)_X + (\rho V^2 + p)_Y = 0. \end{aligned} \tag{5.2.1}$$

In equations (5.2.1), $\rho$, $p$, and $(U, V)$ are density, pressure, and velocity components in $X$ and $Y$ - directions, respectively. The gas is taken to be a more realistic extended Chaplygin gas [138], and the equation of state is presented as

$$p(\rho) = \mathcal{A}\left(\frac{\rho}{1-b\rho}\right)^n - \frac{\mathcal{B}}{\rho^\alpha}\,, \tag{5.2.2}$$

where $\mathcal{A}$ and $\mathcal{B}$ are constants, and $b$ is a constant known as the van der Waals excluded volume. For a better understanding of several Chaplygin gas models, see [14–17]. In equations (5.2.2), $1 \leq< n \leq 3$ is the specific heat ratio, and $0 < \alpha \leq 1$.

A reflection-diffraction phenomenon may be observed when a weak shock hits the right-angled wedge in $(X, Y, t)$ - space shown in Fig. 5.1. In Fig. 5.1$(a)$, a planar shock $C_0$ hits the right-angled rigid wedge at time $t = 0$. The states ahead and

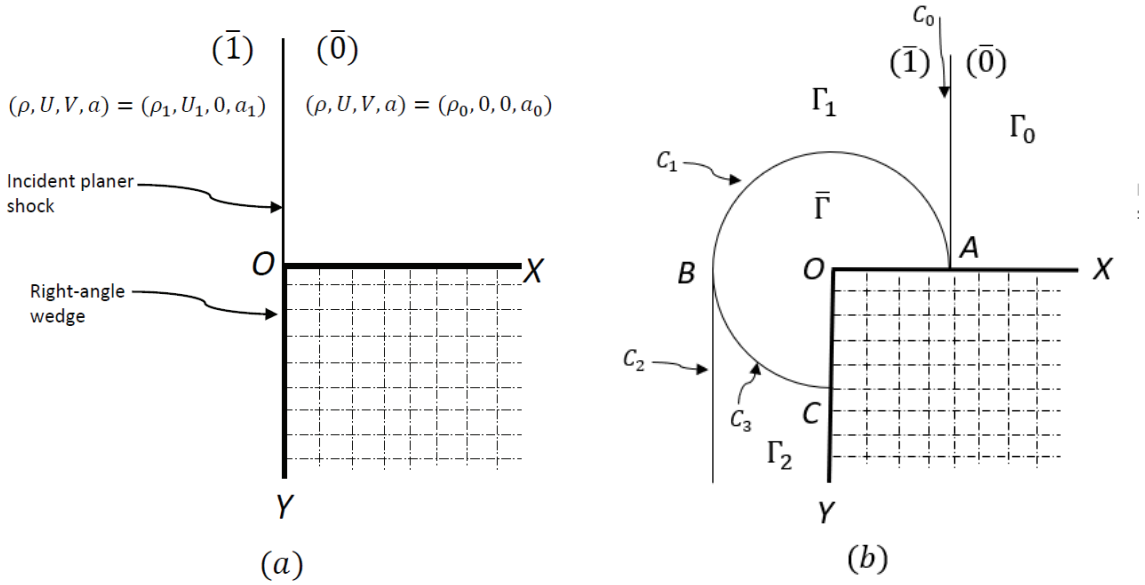


FIGURE 5.1: Incident shock $C_0$ hits the right - angle wedge $(a)$ at $t = 0$ moving along the X - axis, $(b)$ at $t > 0$, the diffraction - reflection phenomena in a self-similar plane $(\xi, \eta)$. $C_1$: diffracted shock, $C_2$: reflected shock, $C_3$: rarefaction wave.

behind the incident shock are represented by $(\bar{0})$ and $(\bar{1})$ in Fig. 5.1$(a)$, and the variables $(\rho, U, V, a)$ are considered to be $(\rho_0, 0, 0, a_0)$ and $(\rho_1, U_1, 0, a_1)$, respectively. In variables $(\rho, U, V, a)$, $a$ represents the speed of sound and is given by $a = \sqrt{\partial p/\partial \rho}$. Moreover, the initial conditions at $t = 0$ may be written as

$$(\rho, U, V, a) = \begin{cases} (\rho_0, 0, 0, a_0), & X > 0,\ Y > 0, \\ (\rho_1, U_1, 0, a_1), & X < 0, \end{cases} \tag{5.2.3}$$

and boundary condition at $Y = 0$ is given by

$$V = 0, \quad X > 0,\ t > 0. \tag{5.2.4}$$

The position of the incident and reflected shocks are given by $X = a_0$ and $X = -a_0$, respectively, in the $XY$-plane. The system of Euler equations (5.2.1) may be transformed into the self-similar plane using the pseudo-variables $\xi = \sqrt{(X^2 + Y^2)}/t$

and $\eta =$ arctan $(Y/X)$ [84]. The transformed system of equations in the self-similar plane is given by

$$\begin{aligned}
&(u-\xi)\rho_\xi + \rho u_\xi + \frac{1}{\xi}(\rho v_\eta + v\rho_\eta + \rho u) = 0,\\
&(u-\xi)u_\xi + \frac{1}{\rho}p_\xi + \frac{1}{\xi}\big(vu_\eta - v^2\big) = 0,\\
&(u-\xi)v_\xi + \frac{1}{\rho}p_\eta + \frac{1}{\xi}\big(vv_\eta - uv\big) = 0.
\end{aligned} \tag{5.2.5}$$

In equations (5.2.5), $u$ and $v$ are velocity components in self-similar flow. The velocity components $u$ and $v$ may be represented as

$$u = U\cos\eta + V\sin\eta, \quad v = -U\sin\eta + V\cos\eta. \tag{5.2.6}$$

The initial and boundary conditions in self-similar flow are obtained by using equations (5.2.6) in equations (5.2.3)-(5.2.4) and given by

$$\lim_{\xi\to\infty}(\rho, u, v, a) = \begin{cases} (\rho_0, 0, 0, a_0), & 0 < \eta < \frac{\pi}{2} \\ (\rho_1, U_1\cos\eta, -U_1\sin\eta, a_1), & \frac{\pi}{2} < \eta < \frac{3\pi}{2} \end{cases}, \tag{5.2.7}$$

and at $\eta = 0$,

$$v = 0, \tag{5.2.8}$$

respectively. The matrix form of system (5.2.5) may be given as

$$\big(A_2(z) - \xi I\big)z_\xi + \frac{1}{\xi}A_1(z)z_\eta + \frac{1}{\xi}A_0(z)z = 0. \tag{5.2.9}$$

In equations (5.2.9), $z$ is a column vector with 3 components and $A_2(z), A_1(z)$ and $A_0(z)$ are $3 \times 3$ matrices defined as follows;

$$z = \begin{bmatrix} \rho \\ u \\ v \end{bmatrix}, A_2 = \begin{bmatrix} u & \rho & 0 \\ a^2/\rho & u & 0 \\ 0 & 0 & u \end{bmatrix}, A_1 = \begin{bmatrix} v & 0 & \rho \\ 0 & v & 0 \\ a^2/\rho & 0 & v \end{bmatrix}, A_0 = \begin{bmatrix} 0 & \rho & 0 \\ 0 & 0 & -v \\ 0 & -v & 0 \end{bmatrix}.$$

It is assumed that a planar shock hits the right-angled rigid wedge at time $t = 0$ (see Fig. 5.1($a$)), and at $t > 0$, it starts propagating along the rigid wedge. When an incident shock $C_0$ hits the wedge, according to linear acoustic [72], a part of incident planar shock is diffracted within a circle of radius $r = a_0 t$, centred at the corner $O$ of the rigid wedge, and the other part is reflected back by the rigid right-angled wedge shown in Fig. 5.1($b$). In Fig. 5.1($b$), the curved portion $AB$ and $BC$ represent the diffracted shock and rarefaction, respectively [73]. The position of the incident shock far away from the corner $O$ of the wedge is given as

$$\xi = a_0 \sec \eta, \tag{5.2.10}$$

and that of reflected shock is

$$\xi = -a_0 \sec \eta. \tag{5.2.11}$$

Here $a_0 = \sqrt{\mathcal{A}}\rho_0^{(n-1)/2}(n(1-b')^{(-n-1)} + \alpha B')^{1/2}$, $b' = b\rho_0$ and $B' = \mathcal{B}/(\mathcal{A}\rho_0^{\alpha+n})$. The domain of the entire flow is divided into four regions $\Gamma_0$, $\Gamma_1$, $\Gamma_2$ and $\bar{\Gamma}$ by the reflection-diffraction phenomenon of planar incident shock (see Fig. 5.1($b$)). The region $\bar{\Gamma}$ is called the diffracted region. The entire region of flow in the self-similar plane is given by

$$\Gamma = \Gamma_0 \cup \Gamma_1 \cup \Gamma_2 \cup \overline{\Gamma},$$

where

$$\Gamma_0 = \{(\xi,\eta)|\ \xi > a_0 \sec\eta, 0 < \eta < \pi/2\},$$

$$\Gamma_1 = \{(\xi,\eta)|\ a_0 < \xi < a_0 \sec\eta, 0 < \eta < \pi\} \cup \{(\xi,\eta)|\xi < -a_0 \sec\eta, \pi < \eta < 3\pi/2\},$$

$$\Gamma_2 = \{(\xi,\eta)|\ -a_0 \sec\eta < \xi < -a_0, \pi < \eta < 3\pi/2\},$$

$$\overline{\Gamma} = \{(\xi,\eta)|\ \xi < a_0, 0 < \eta < 3\pi/2\}.$$

In Fig. 5.1, $C_0$ is the incident shock, which hits the right-angled wedge at A. In this context, the segment BC serves as the sonic curve, defined by $\xi = a_0$, where a smooth transition occurs from the supersonic region $\Gamma_2$ to the subsonic region $\overline{\Gamma}$. In contrast, AB is the free boundary associated with the diffraction of the planar shock, across which the flow abruptly shifts from the supersonic region $\Gamma_1$ to $\overline{\Gamma}$ near the origin. While the flow remains constant in regions $\Gamma_1$ and $\Gamma_2$, it exhibits a pseudo-subsonic behaviour in $\overline{\Gamma}$.

The hyperbolic Euler system (5.2.1) dictates the overall flow pattern. However, when expressed in self-similar coordinates $(\xi,\eta)$, the flow is described by mixed-type equations (5.2.9), which transitions from elliptic to hyperbolic as the point $(\xi,\eta)$ moves from the origin toward infinity. Consequently, one must solve the free boundary value problem for a degenerate elliptic equation to accurately determine the entire flow field and its associated wave structure.

## 5.3 R-H conditions for the incident and reflected shock and asymptotic expansions

This section describes the R-H conditions to find the states ahead and behind the reflected shock. Moreover, asymptotic expansions are presented for both states.

Recall that the state ahead of the incident shock is $(\rho_0, 0, 0, a_0)$. It is assumed that $(\rho_1, u_1, v_1, a_1)$ and $(\rho_2, u_2, v_2, a_2)$ denote the immediate state behind the incident and reflected shock. If $\xi = f(\eta)$ is the shock curve, then R-H conditions are given by

$$\begin{aligned} df/d\eta[\rho] &= \mu[\rho U] + \nu[\rho V], \\ df/d\eta[\rho U] &= \mu[\rho U^2 + p] + \nu[\rho UV], \\ df/d\eta[\rho V] &= \mu[\rho V^2 + p] + \nu[\rho UV]. \end{aligned} \tag{5.3.1}$$

In equation (5.3.1), $df/d\eta$ is the shock speed and [.] denotes the jump across the shock, and $(\mu, \nu)$ represents the normal vector to the shock front. The R-H conditions in self-similar flow are found as

$$\begin{aligned} [\rho(u-\xi)]\xi d\eta &= [\rho v]d\xi, \\ [\rho(u-\xi)^2 + p]\xi d\eta &= [\rho(u-\xi)v]d\xi, \\ [\rho(u-\xi)v]\xi d\eta &= [\rho v^2 + p]d\xi. \end{aligned} \tag{5.3.2}$$

To find expressions for state - $(\overline{1})$ variables $U_1$ and $V_1$ in $XY$ - plane, the use of equation (6.2.1) is made in equation (5.3.1) and it is obtained as

$$U_1 = \sqrt{\frac{(p_1 - p_0)(\rho_1 - \rho_0)}{\rho_1 \rho_0}}, \quad V_1 = 0. \tag{5.3.3}$$

A non-dimensional parameter $\delta > 0$ is considered such that,

$$\rho_1 = \rho_0(1+\delta). \tag{5.3.4}$$

Making use of equations (5.2.2), (5.2.6), (5.2.10), (5.3.3) and (5.3.4), as $\delta \to 0$ the asymptotic expansions of variables of state - $(\overline{1})$ may be written as

$$\begin{aligned}
\frac{\rho_1}{\rho_0} &= 1 + \rho_1^{(1)}\delta, \\
\frac{u_1}{\sigma_0} &= u_1^{(1)}\delta + u_1^{(2)}\delta^2 + \mathcal{O}(\delta^3), \\
\frac{v_1}{\sigma_0} &= v_1^{(1)}\delta + v_1^{(2)}\delta^2 + \mathcal{O}(\delta^3), \\
\frac{a_1}{\sigma_0} &= 1 + a_1^{(1)}\delta + a_1^{(2)}\delta^2 + \mathcal{O}(\delta^3), \\
\frac{\xi}{\sigma_0} &= K_0 \sec\eta + \mathcal{O}(\delta),
\end{aligned} \tag{5.3.5}$$

where $\rho_1^{(1)}, u_1^{(1)}, u_1^{(2)}, v_1^{(1)}, v_1^{(2)}, a_1^{(1)}$ and $a_1^{(2)}$ are unknowns and $K_0 = \left(\frac{n}{(1-b')^{n+1}} + \alpha B'\right)^{1/2}$, $\sigma_0 = (\mathcal{A}\rho_0^{n-1})^{1/2}$, $b' = b\rho_0$, $B' = \mathcal{B}/(\mathcal{A}\rho_0^{(\alpha+n)})$ and $p_0' = An\rho_0^{n-1}(1 - b\rho_0)^{-(n+1)} + \alpha\rho_0^{-(\alpha+1)}$. In equations (5.3.1) and (5.3.5), making use of equations (5.3.3) and (5.3.4), the following expressions of unknowns may be obtained

$$\begin{aligned}
&\varrho_1^{(1)} = 1, \quad u_1^{(1)} = K_0\cos\eta, \quad u_1^{(2)} = K_0\cos\eta\frac{n(n-3+4b') - \alpha(\alpha+3)B'(1-b')^{n+2}}{4(1-b')(n+\alpha B'(1-b')^{n+1})} \\
&v_1^{(1)} = -K_0\sin\eta, \quad v_1^{(2)} = -K_0\sin\eta\frac{n(n-3+4b') - \alpha(\alpha+3)B'(1-b')^{n+2}}{4(1-b')(n+\alpha B'(1-b')^{n+1})}
\end{aligned}$$

$$a_1^{(1)} = \frac{\rho_0}{2\sqrt{p_0'}}\left\{A\,n\,\rho_0^{n-2}(1-b\rho_0)^{-(n+2)}\big((n-1)+2b\rho_0\big) - \alpha(\alpha+1)B\,\rho_0^{-(\alpha+2)}\right\},$$

$$a_1^{(2)} = \frac{\rho_0^2}{4\sqrt{p_0'}}\Bigg\{A\,n\,\rho_0^{n-3}(1-b\rho_0)^{-(n+3)}\Big(n^2-3n+2+6bn\rho_0-6b\rho_0+6b^2\rho_0^2\Big) + \alpha(\alpha+1)(\alpha+2)B\,\rho_0^{-(\alpha+3)}\Bigg\} - \frac{\rho_0^2}{8(p_0')^{3/2}}\Bigg\{A\,n\,\rho_0^{n-2}(1-b\rho_0)^{-(n+2)}\big((n-1)+2b\rho_0\big) - \alpha(\alpha+1)B\,\rho_0^{-(\alpha+2)}\Bigg\}^2.$$

To obtain the variables of state - $(\overline{2})$, the following asymptotic expansions are considered:

$$\begin{aligned}
\frac{\rho_2}{\rho_0} &= 1+\rho_2^{(1)}\delta+\mathcal{O}(\delta^2),\\
\frac{u_2}{\sigma_0} &= u_2^{(1)}\delta+u_2^{(2)}\delta^2+\mathcal{O}(\delta^2),\\
\frac{v_2}{\sigma_0} &= v_2^{(1)}\delta+v_2^{(2)}\delta^2+\mathcal{O}(\delta^2),\\
\frac{\xi}{\sigma_0} &= -K_0\sec\eta+\mathcal{O}(\delta).
\end{aligned} \tag{5.3.6}$$

To find the expressions of unknowns $\rho_2^{(1)}, u_2^{(1)}, u_2^{(2)}, v_2^{(1)}$ and $v_2^{(2)}$ in equation (5.3.6), equations (5.3.5) and (5.3.6) are used in R-H conditions in self-similar flow (5.3.2) and are found as;

$$\begin{aligned}
&\rho_2^{(1)}=2,\quad u_2^{(1)}=0,\\
&u_2^{(2)}=K_0\cos\eta\left[\frac{n(n-3+6b')-\alpha(\alpha+3)B'(1-b')^{n+2}}{4(1-b')(n+\alpha B'(1-b')^{n+1}}\right],\\
&v_2^{(1)}=0,\quad v_2^{(2)}=-K_0\sin\eta\left[\frac{n(n-3+6b')-\alpha(\alpha+3)B'(1-b')^{n+2}}{4(1-b')(n+\alpha B'(1-b')^{n+1}}\right],
\end{aligned}$$

Note that, while solving equation (5.3.2), coefficients of $\delta$ of order 1 and 2 are

compared. From equations $(5.3.5)_1$ and $(5.3.6)_1$, it is seen that the first-order approximation of the variable $\rho$ is given by

$$\rho_i^{(1)}(\xi,\eta) = \begin{cases} 1, & (\xi,\eta) \in \Gamma_1 \\ 2, & (\xi,\eta) \in \Gamma_2 \end{cases}, \quad i = 1, 2. \tag{5.3.7}$$

In equation (5.3.7), $\rho_i^{(1)}(\xi,\eta)$ is piecewise constant in the region $\Gamma \setminus \bar{\Gamma}$. In [83], the asymptotic expansions were obtained to find real gas effects for a van der Waals-type equation of state when a planar shock hits the right-angle wedge. It may be observed that the entropy condition did not play any significant role in finding the state variables behind and ahead of the reflected shock. The states behind and ahead of the reflected shock may be obtained by using the R-H conditions (5.3.1) and (5.3.2) for the given equation of state (5.2.2).

## 5.4 Behaviour of asymptotic expansions in the diffracted region $\bar{\Gamma}$

In this section, the asymptotic behaviour of the solution in the diffracted region is analyzed. To obtain the approximate solution in the diffracted region, a dimensionless parameter $\overline{\xi} = \xi/a_0$, is introduced, and the asymptotic expansions of variables $(\rho, u, v)$ are expressed as

$$\begin{aligned} \frac{\rho}{\rho_0} &= 1 + \overline{\rho_1}\delta + \overline{\rho_2}\delta^2 + \mathcal{O}(\delta^3), \\ \frac{u}{\sigma_0} &= \overline{u_1}\delta + \overline{u_2}\delta^2 + \mathcal{O}(\delta^3), \\ \frac{v}{\sigma_0} &= \overline{v_1}\delta + \overline{v_2}\delta^2 + \mathcal{O}(\delta^3). \end{aligned} \tag{5.4.1}$$

Using equation (5.4.1) in the system of equation (5.2.9), the following three equations are obtained for first-order approximation

$$\begin{aligned}
&(\overline{\xi})^2(\overline{\rho_1})_{\overline{\xi}} - \overline{\xi}(\overline{u_1})_{\overline{\xi}} - (\overline{v_1})_{\eta} + K_0\overline{u_1} = 0,\\
&(\overline{\rho_1})_{\overline{\xi}} - \overline{\xi}(\overline{u_1})_{\overline{\xi}} = 0,\\
&(\overline{\xi})^2(\overline{u_1})_{\overline{\xi}} - (\overline{\rho_1})_{\eta} = 0.
\end{aligned} \tag{5.4.2}$$

Solving equation (5.4.2), a partial differential equation is found and given as

$$(\overline{\xi})^2\left[(1-\overline{\xi}^2)(\overline{\rho_1})_{\overline{\xi}}\right]_{\overline{\xi}} + (\overline{\rho_1})_{\eta\eta} + \overline{\xi}(\overline{\rho_1})_{\overline{\xi}} = 0\ . \tag{5.4.3}$$

On introducing a new variable $\overline{r} = \frac{\overline{\xi}}{1+\sqrt{1-\overline{\xi}^2}}$, equation (5.4.3) leads to the following Laplace equation in variables $(\overline{r}, \eta)$,

$$\overline{r}\left(\overline{r}(\overline{\rho_1})_{\overline{r}}\right)_{\overline{r}} + (\overline{\rho_1})_{\eta\eta} = 0\ . \tag{5.4.4}$$

The solution of equation (5.4.4) is found in [72] and valid for $\overline{r} \leq 1, 0 \leq \eta \leq 3\pi/2$, given by

$$\overline{\rho_1} = 1 + \frac{1}{\pi}\arctan\left(\frac{\sqrt{3}\left(1-\overline{r}^{4/3}\right)}{1+\overline{r}^{4/3}+4\overline{r}^{2/3}\cos(2\eta/3)}\right). \tag{5.4.5}$$

From equation (5.4.5), it may be observed that if $\overline{\rho_1}$ does not exist at $\overline{r} = 1$ or at $\overline{\xi} = 1$. Therefore, $\overline{\xi} = 1$ or $\xi = a_0$ is the point of singularity. The solution $\overline{\rho_1}$ is invalid in the whole region $\overline{\Gamma}$. As one moves along the boundary, $C_1$ i.e. along the diffracted wavefront, the normal derivative of the linear solution, $\overline{\rho_1}$ i.e. $\overline{\rho_{1\overline{r}}}$ is unbounded, whereas both the normal and tangential derivatives $\overline{\rho_{1\overline{r}}}$ and $\overline{\rho_{1\eta}}$, respectively, are unbounded at the triple point $B$, which forces us to include the non-linear effects at those points where the singularity occurs. For the equation of state (5.2.2), the singularity is found at $\overline{\xi} = 1$ or $\xi = a_0$. To find the nonlinear effect

near $\overline{\xi} = 1$, following expansion of equation (5.4.5) may be considered for $j = 1, 2$ as

$$\overline{\rho_1} = \rho_1^{(j)} + \left(\frac{2}{3}\right)^{1/2} \frac{1}{\pi} \frac{2}{1 + 2\cos(2\eta/3)} \left(1 - \overline{\xi}\right)^{1/2} + \mathcal{O}\left(1 - \overline{\xi}\right) + \mathcal{O}\left(\frac{\delta^2}{(1 - \overline{\xi})^{1/2}}\right) , \quad (5.4.6)$$

Therefore, from equations (5.4.1) and (5.4.6), the expression of $\rho$ is given by

$$\frac{\rho}{\rho_0} = 1 + \rho_1^{(j)}\delta + \left(\frac{2}{3}\right)^{1/2} \frac{\delta}{\pi} \frac{2}{1 + 2\cos(2\eta/3)} \left(1 - \frac{\xi}{a_0}\right)^{1/2} + \delta\mathcal{O}\left(1 - \frac{\xi}{a_0}\right) + \delta^2\mathcal{O}\left(\left(1 - \frac{\xi}{a_0}\right)^{-1/2}\right) . \quad (5.4.7)$$

## 5.5 Behaviour of nonlinear expansions on curve ABC

In this section, nonlinear approximations are considered to analyze the effect of singularity on diffraction-reflection phenomena. Nonlinear approximations play a significant role in the solution near the point of singularity.

It may be observed in equation (5.4.5) that the singularity is found at $\xi = a_0$. Since $det(A_2 - \xi I) = 0$, in the system of equation (5.2.9), it may be noticed that the system of equation (5.2.9) shows degeneracy at point $\xi = u_0 + a_0, u_0, u_0 - a_0$ i.e. $\xi = a_0, 0, -a_0$. In order to study the nonlinear effect, $\xi = a_0$ the expression of $\xi$ near $a_0$ may be taken as

$$\xi(a_0) = a_0(1 + a_1^{(j)}\delta + u_1^{(j)}\delta) + \delta^2\omega \, . \quad (5.5.1)$$

In equation (5.5.1), the parameter $\omega$ is taken into account to show the nonlinearity effect, and its expansion is given by

$$\omega = \left(\xi - a_0\right)\frac{1}{\delta^2} + \mathcal{O}\left(\frac{1}{\delta}\right) . \quad (5.5.2)$$

For $\xi = a_0$ and $\eta(\neq \pi)$, arc ABC may be divided into two parts $C_1$ and $C_3$, which represent the diffracted shock and expansion wave, respectively (see Fig. 5.1(b)). The expansions on the boundaries $C_1$, and $C_3$ may be expressed as

$$\begin{aligned}
\frac{\rho}{\rho_0} &= 1 + \rho_1^{(j)}\delta + (\tilde{\rho} - \rho_2^{(j)})\delta^2 + \mathcal{O}(\delta^3),\\
\frac{u}{\sigma_0} &= u_1^{(j)}\delta + (\tilde{u} - u_2^{(j)})\delta^2 + \mathcal{O}(\delta^3),\\
\frac{v}{\sigma_0} &= v_1^{(j)}\delta + (\tilde{v} - v_2^{(j)})\delta^2 + \mathcal{O}(\delta^3),\\
\frac{a}{\sigma_0} &= 1 + a_1^{(j)}\delta + (\tilde{a} - a_2^{(j)})\delta^2 + \mathcal{O}(\delta^3)\ .
\end{aligned} \tag{5.5.3}$$

In equation (5.5.3), $\tilde{\rho} = \tilde{\rho}(\eta,\omega), \tilde{u} = \tilde{u}(\eta,\omega), \tilde{v} = \tilde{v}(\eta,\omega)$ and $\tilde{a} = \tilde{a}(\eta,\omega)$ are functions of $\omega$ and $\eta$ and superscript $(j)$ corresponds to states - $(\overline{1})$ and $(\overline{2})$. Using equation (5.5.3), in equation (5.2.9), and using $\mathcal{O}(1)$, $\mathcal{O}(\delta)$ and $\mathcal{O}(\delta^2)$ equations, the following partial differential equation may be derived,

$$\left\{\sigma_0 K_0 \mathcal{K}\frac{(\tilde{\rho} - \rho_2^{(j)})^2}{2} + 2(\mathcal{C} - \omega)(\tilde{\rho} - \rho_2^{(j)})\right\}(\tilde{\rho} - \rho_2^{(j)})_\omega + 3(\tilde{\rho} - \rho_2^{(j)}) = 0, \tag{5.5.4}$$

where $\mathcal{K}$, $\mathcal{C}$ is given by

$$\mathcal{K} = \frac{n(n-1+2b') + \alpha B'(1-b')^{n+2}}{2(1-b')(n+\alpha B'(1-b')^{n+1})}, \tag{5.5.5}$$

$$\begin{aligned}
\mathcal{C} = \sigma_0 K_0 \Bigg\{ & \frac{n(n-1+2b') + \alpha B'(1-b')^{n+2}}{2(1-b')(n+\alpha B'(1-b')^{n+1})}\rho_i^{(2)} + u_i^{(2)} - \frac{v_i^{(2)} u_{i\eta}^{(2)}}{2} \\
& - \frac{B'^2\alpha^2(\alpha+1)^2(1-b')^{2n+2}}{8(n+\alpha B'(1-b')^{n+1})^2}\Bigg\}\rho_i^{(1)2} \\
& + \sigma_0 K_0 \frac{n(n-1)(n-2)(1-b')^2 + (n+1)(n+2)b'^2 + 2(n-1)(n+1)b'(1-b')}{(1-b')^2(n+\alpha B'(1-b')^{n+1})}\rho_i^{(1)2}\ .
\end{aligned} \tag{5.5.6}$$

The boundary condition may be obtained by using the fact that $\frac{\rho}{\rho_0} \to 1+\rho_1^{(j)}\delta$ as $\omega \to \infty$. Therefore, the following boundary condition is obtained from equation $(5.5.3)_1$

$$(\tilde{\rho} - \rho_2^{(j)}) \to 0 \ \text{ as } \ \omega \to \infty \, . \tag{5.5.7}$$

Now, for solving the partial differential equation (5.5.4), by integrating it, the solution may be found as

$$(\tilde{\rho} - \rho_2^{(j)})^2 = \frac{1}{I_0(\eta)}(\omega - \mathcal{C}) - \frac{1}{I_0(\eta)}\left(\sigma_0 K_0 \mathcal{K}(\tilde{\rho} - \rho_2^{(j)})\right) . \tag{5.5.8}$$

In equation (5.5.8), $I_0(\eta)$ is the constant of integration. Boundary conditions (5.5.7), ensures that there exist a value of $\omega = \omega_s$, such that for $\omega > \omega_s$, $\tilde{\rho} = \rho_2^{(j)}$. For $I_0(\eta) < 0$ and $\omega < \omega_s$, there may be a shock or an expansion wave. It may be observed that for $I_0(\eta) > 0$, equation (5.5.8) represents a parabola in $(\tilde{\rho}, \omega)$ - plane with two branches approaching $\pm\infty$ i.e. $\tilde{\rho} \to \pm\infty$ as $\omega \to \infty$, a violation of boundary condition (5.5.7). For shock, the R-H condition at $\omega = \omega_s$ is found as

$$\begin{aligned} &\left(\sigma_0 K_0 \mathcal{K}\frac{(\tilde{\rho} - \rho_2^{(j)})^2}{2} + 2(\mathcal{C} - \omega)(\tilde{\rho} - \rho_2^{(j)})\right)_{\omega=\omega_s^+} \\ &- \left(\sigma_0 K_0 \mathcal{K}\frac{(\tilde{\rho} - \rho_2^{(j)})^2}{2} + 2(\mathcal{C} - \omega)(\tilde{\rho} - \rho_2^{(j)})\right)_{\omega=\omega_s^-} = 0 \, . \end{aligned} \tag{5.5.9}$$

For $\omega > \omega_s$, $\tilde{\rho} = \rho_2^{(j)}$ that is, $\tilde{\rho}(\omega_s^+) = \rho_2^{(j)}$. Therefore equation (5.5.9) may be written as

$$\left(\sigma_0 K_0 \mathcal{K}\frac{(\tilde{\rho} - \rho_2^{(j)})}{2} + 2(\mathcal{C} - \omega)\right)_{\omega=\omega_s^-} = 0 \, . \tag{5.5.10}$$

From equation (5.5.10), the value of $\tilde{\rho}(\omega_s^-)$ may be calculated as

$$\tilde{\rho}(\omega_s^-) = -\frac{4\mathcal{C}}{\sigma_0 K_0} + \rho_2^{(j)} + \frac{4\omega_s}{\sigma_0 K_0} \, . \tag{5.5.11}$$

It may be noticed in equation (5.5.11), for $\mathcal{C} > \omega_s$, $\tilde{\rho}(\omega_s^-) > 0$. Using equation (5.5.8), the value of $\omega_s$ for shock may be found as

$$\omega_s = \mathcal{C} - \frac{3}{I_0(\eta)}\left(\frac{\sigma_0 K_0 \mathcal{K}}{4}\right)^2 . \tag{5.5.12}$$

With the help of equation (5.5.8), (5.5.12), for a given value of $I_0(\eta)$ and for small values of $\mathcal{C}$, $\tilde{\rho}$ is given by

$$\tilde{\rho} \approxeq \pm\left(\frac{\omega}{I_0(\eta)}\right)^{1/2} \text{ as } \omega \to -\infty . \tag{5.5.13}$$

Making use of equation (5.5.2) and (5.5.13), the expansion of $\tilde{\rho}$ is obtained as

$$\tilde{\rho} = \left\{\frac{-a_0}{I_0(\eta)}\left(1 - \frac{\xi}{a_0}\right)\frac{1}{\delta^2} + \mathcal{O}\left(\frac{1}{\delta}\right)\right\}^{1/2} . \tag{5.5.14}$$

The nonlinear expansion of $\rho$ is given by

$$\frac{\rho}{\rho_0} = 1 + \rho_1^{(j)}\delta \pm \delta\left\{\frac{-a_0}{I_0(\eta)}\left(1 - \frac{\xi}{a_0}\right)\right\}^{1/2} + \mathcal{O}(\delta^2) . \tag{5.5.15}$$

In order to find the value of $I_0(\eta)$, from the comparison of equations (5.4.7) and (5.5.15), it is obtained that for $\delta << 1 - \frac{\xi}{a_0} << 1$,

$$\left(\frac{2}{3}\right)^{1/2}\frac{1}{\pi}\frac{2}{1 + 2\cos(2\eta/3)} = \begin{cases} \left(\frac{-a_0}{I_0(\eta)}\right)^{1/2}, & \eta < \pi, \\ -\left(\frac{-a_0}{I_0(\eta)}\right)^{1/2}, & \eta > \pi. \end{cases} \tag{5.5.16}$$

From equation (5.5.16), it may be noticed that $1/I_0(\eta)$ exists for all values of $\eta(\neq \pi)$ and given by

$$\frac{1}{I_0(\eta)} = \frac{-2}{3a_0}\frac{4}{\pi^2(1 + 2\cos(2\eta/3))^2} . \tag{5.5.17}$$

From equations (5.5.12) and (5.5.17), the location of the diffracted shock for $\eta(\neq \pi)$ is given by

$$\omega_s = \mathcal{C} + \frac{1}{8}\frac{\sigma_0 K_0}{\pi^2(1+2\cos(2\eta/3))^2}\left\{\frac{n(n-1+2b')+\alpha B'(1-b')^{n+2}}{(1-b')(n+\alpha B'(1-b')^{n+1})}\right\}^2 . \tag{5.5.18}$$

Solution of partial differential equation (5.4.3) with boundary condition (5.5.7), may be obtained with the help of equation (5.5.8) and (5.5.18) and may be considered for $0 < \eta < \pi$ and $\pi < \eta < 3\pi/2$ separately.

(i) When $0 < \eta < \pi$, the wavefront represents diffracted shock AB ($C_1$), since the density increases across the shock, the jump is given by

$$\tilde{\rho} - \rho_2^{(j)} = -\frac{\sigma_0 K_0 \mathcal{K}}{2I_0(\eta)} + \frac{1}{2I_0(\eta)}\sqrt{(\sigma_0 K_0 \mathcal{K})^2 - 4I_0(\eta)(\mathcal{C}-\omega)} . \tag{5.5.19}$$

(ii) When $\pi < \eta < 3\pi/2$, the wavefront represents a rarefaction BC ($C_3$), since the density decreases across the expansion, the jump is given by

$$\tilde{\rho} - \rho_2^{(j)} = -\frac{\sigma_0 K_0 \mathcal{K}}{2I_0(\eta)} - \frac{1}{2I_0(\eta)}\sqrt{(\sigma_0 K_0 \mathcal{K})^2 - 4I_0(\eta)(\mathcal{C}-\omega)} . \tag{5.5.20}$$

It may be noticed that the jumps presented in equation (5.5.19) and (5.5.20) show the strength of the shock wave and rarefaction wave, respectively, and are shown by AB and BC in Fig. 5.1(b). Positive and negative roots in equations (5.5.19) and (5.5.20) show an increase in density across the shock and a decrease in density for the rarefaction wave, respectively.

## 5.6 Asymptotic expansion for a shock coming off a wedge and shock incident on a screen

In this section, equation (5.4.2) is solved for two different scenarios: (i) when a weak shock is coming off a wedge [73], and (ii) when a weak shock hits the screen [73]. The jump in diffracted shocks is obtained for both cases.

### 5.6.1 Shock coming off a wedge

When shock comes off a wedge, the behaviour of asymptotic expansion (5.4.7) in the diffracted region is given by

$$\left(\frac{\rho}{\rho_0}\right)_w = 1+\rho_1^{(j)}\delta-\left(\frac{2}{3}\right)^{1/2}\frac{\delta}{\pi}\frac{2}{1+2\cos(2\eta/3)}\left(1-\frac{\xi}{a_0}\right)^{1/2}+\delta\mathcal{O}\left(1-\frac{\xi}{a_0}\right)+\delta^2\mathcal{O}\left(\left(1-\frac{\xi}{a_0}\right)^{-1/2}\right). \tag{5.6.1}$$

Suffix '$w$' in equation (5.6.1) corresponds to the phenomenon of shock coming off a wedge. In this case, equation (5.5.16) is presented as

$$\left(\frac{2}{3}\right)^{1/2}\frac{1}{\pi}\frac{2}{1+2\cos(2\eta/3)} = \begin{cases} -\left(\frac{-a_0}{I_0(\eta)}\right)^{1/2}, & \eta<\pi, \\ \left(\frac{-a_0}{I_0(\eta)}\right)^{1/2}, & \eta>\pi, \end{cases} \tag{5.6.2}$$

and the jump $\tilde{\rho}-\rho_2^{(j)}$ may be found for $0<\eta<\pi$ and $\pi<\eta<3\pi/2$.

$(i)_w$ when $0<\eta<\pi$, the wavefront represents a rarefaction, and the jump is given by

$$(\tilde{\rho}-\rho_2^{(j)})_w = -\frac{\sigma_0 K_0\mathcal{K}}{2I_0(\eta)}-\frac{1}{2I_0(\eta)}\sqrt{(\sigma_0K_0\mathcal{K})^2-4I_0(\eta)(\mathcal{C}-\omega)}\,. \tag{5.6.3}$$

$(ii)_w$ When $\pi < \eta < 3\pi/2$, the wavefront represents a shock wave, and the jump is given by

$$(\tilde{\rho} - \rho_2^{(j)})_w = -\frac{\sigma_0 K_0 \mathcal{K}}{2I_0(\eta)} + \frac{1}{2I_0(\eta)}\sqrt{(\sigma_0 K_0 \mathcal{K})^2 - 4I_0(\eta)(\mathcal{C} - \omega)}\,. \tag{5.6.4}$$

### 5.6.2 Shock incident on a screen

When a shock hits a screen, the behaviour of asymptotic expansion (5.4.7) in the diffracted region is given by

$$\left(\frac{\rho}{\rho_0}\right)_s = 1 + \rho_1^{(j)}\delta + \frac{\delta}{\pi}\frac{\cos(\eta/2)}{\cos(\eta)}\left(1 - \frac{\xi}{a_0}\right)^{1/2} + \delta\mathcal{O}\left(1 - \frac{\xi}{a_0}\right) + \delta^2\mathcal{O}\left(\left(1 - \frac{\xi}{a_0}\right)^{-1/2}\right). \tag{5.6.5}$$

where suffix '$s$' in (5.6.5) represents the phenomenon shock hitting a screen. In this case, equation (5.5.16) is presented as

$$\frac{1}{\pi}\frac{\cos\eta/2}{\cos\eta} = \begin{cases} \left(\frac{-a_0}{I_0(\eta)}\right)^{1/2}, & 0 < \eta < \pi/2 \text{ and } \pi \leq \eta < 3\pi/2 \\ -\left(\frac{-a_0}{I_0(\eta)}\right)^{1/2}, & \pi/2 < \eta \leq \pi \text{ and } 3\pi/2 < \eta < 2\pi \end{cases} \tag{5.6.6}$$

and the jump $\tilde{\rho} - \rho_2^{(j)}$ may be found for $0 < \eta < \pi$ and $\pi < \eta < 3\pi/2$.

$(i)_s$ when $0 < \eta < \pi/2$ and $\pi \leq \eta < 3\pi/2$, the wavefront represents a rarefaction, and the jump is given by

$$(\tilde{\rho} - \rho_2^{(j)})_s = -\frac{\sigma_0 K_0 \mathcal{K}}{2I_0(\eta)} - \frac{1}{2I_0(\eta)}\sqrt{(\sigma_0 K_0 \mathcal{K})^2 - 4I_0(\eta)(\mathcal{C} - \omega)}\,. \tag{5.6.7}$$

$(ii)_s$ When $\pi/2 < \eta \leq \pi$ and $3\pi/2 < \eta < 2\pi$, the wavefront represents a shock wave, and the jump is given by

$$(\tilde{\rho} - \rho_2^{(j)})_s = -\frac{\sigma_0 K_0 \mathcal{K}}{2I_0(\eta)} + \frac{1}{2I_0(\eta)}\sqrt{(\sigma_0 K_0 \mathcal{K})^2 - 4I_0(\eta)(\mathcal{C} - \omega)}\,. \tag{5.6.8}$$

## 5.7 Behaviour of nonlinear expansions near singular point $B(a_0, \pi)$

This section obtains the nonlinear asymptotic expansion at the intersection B of diffracted shock ($C_1$), reflected shock ($C_2$), and expansion wave profiles ($C_3$) boundaries. It is observed that the expansions derived in Section 5 to represent the solution near the diffracted front are not valid near the singular point since the shock strength and position $\omega$ are found to approach infinity as $\eta \to \pi$. This section presents an expansion to obtain the solution in the neighborhood of the singular point.

To present an expansion near the singular point B (see Fig. 5.1(b)), the following new variables are introduced [135]

$$\mathcal{R} = \frac{1 - \overline{\xi}}{\delta}, \quad \text{and} \quad \Theta = \begin{cases} \frac{(\pi - \eta)}{\delta^{1/2}}, & \eta < \pi \ \text{ in } C_1, \\ \frac{(\eta - \pi)}{\delta^{1/2}}, & \eta > \pi \ \text{ in } C_2 \cup C_3. \end{cases} \tag{5.7.1}$$

With the help of variables defined in equation (5.7.1), the expansion near point B may be presented as

$$\begin{aligned}
\frac{\rho}{\rho_0} &= 1 + \check{\rho}(R,\Theta)\delta + \check{\check{\rho}}(R,\Theta)\delta^{3/2} + \mathcal{O}(\delta^2),\\
\frac{u}{\sigma_0} &= \check{u}(R,\Theta)\delta + \check{\check{u}}(R,\Theta)\delta^{3/2} + \mathcal{O}(\delta^2),\\
\frac{v}{\sigma_0} &= \check{v}(R,\Theta)\delta + \check{\check{v}}(R,\Theta)\delta^{3/2} + \mathcal{O}(\delta^2),\\
\frac{a}{\sigma_0} &= K_0 + \check{a}\delta + \check{\check{a}}\delta^{3/2} + \mathcal{O}(\delta^2)\ .
\end{aligned} \tag{5.7.2}$$

By substituting the expansions from equation (5.7.2) into the matrix formulation of equation (5.2.9) and systematically collecting terms of orders $\mathcal{O}(1)$, $\mathcal{O}(\delta^{1/2})$, and $\mathcal{O}(\delta)$, we obtain the following system of equations:

$$\begin{aligned}
&a_0\check{v}_{\mathcal{R}} = \check{\rho}_{\Theta},\\
&2\Big(a_0(\check{\rho} - \rho_i^{(1)}) + u_i^{(1)} - \mathcal{R} + a_0\check{a}\Big)\check{\rho}_{\mathcal{R}} + \check{\check{v}}_{\Theta} + \check{\rho} - \rho_i^{(1)} + u_i^{(1)} = 0,
\end{aligned} \tag{5.7.3}$$

where

$$\check{a} = K_0\frac{(n(n-1+2b') + \alpha B'(1-b')^{n+2})\check{\rho}}{2(1-b')(n+\alpha B'(1-b')^{n+1})}.$$

To obtain the reflected and diffracted shock positions, consider that $\mathcal{C}_2 = \mathcal{C}_2(\Theta)$ and $\mathcal{C}_1 = \mathcal{C}_1(\Theta)$, be the positions of reflected and diffracted shocks, respectively. The above system of equation (5.7.3) becomes

$$\frac{d\mathcal{C}_k}{d\Theta}[\check{\rho}] + a_0[\check{\check{v}}] = 0, \tag{5.7.4}$$

$$\frac{d\mathcal{C}_k}{d\Theta}[\check{\check{v}}] + 2\mathcal{C}_k - [\check{\rho}] + A_0[\check{\rho}^2] = 0, \tag{5.7.5}$$

where $k = 1, 2$ and $A_0 = a_0\check{a}$ and $\mathcal{C}_k = \mathcal{R} - a_0(u_i^{(1)} - \rho_i^{(1)})$. With the help of equation (5.7.4) and (5.7.5), we get

$$\left(\frac{d\mathcal{C}_k}{d\Theta}\right)^2 - 2a_0\mathcal{C}_k + A_0\overline{\rho} = 0, \quad k \in \{1, 2\}, \tag{5.7.6}$$

where $\overline{\rho}$ denotes the average value of $\check{\rho}$ on either side of the discontinuity $\mathcal{C}_k = \mathcal{C}_k(\Theta)$.

Note that the variables considered in (5.7.1), which connects region $\overline{\Gamma}$ and the singular point B, have the following relation

$$\frac{\mathcal{R}^2}{\Theta} \to \frac{a_0}{2}, \quad \text{as} \quad \Theta \to \infty. \tag{5.7.7}$$

Therefore, for a real number, $\psi$ the condition on $\check{\rho}$ is given by

$$\lim_{\Theta\to\infty} \check{\rho}\left(\psi a_0\Theta^2/2, \Theta\right) = \lim_{\epsilon\to 0} \overline{\rho_1} = \begin{cases} 1, & \psi > 1 \\ 2, & 0 < \psi < 1 \\ 2 - \frac{1}{\pi}\arctan\sqrt{-\psi}, & \psi < 0 \end{cases}. \tag{5.7.8}$$

Solving the equation (5.7.6) using the boundary condition (5.7.8), the locations of reflected and diffracted shocks are given by

$$\mathcal{C}_2(\Theta) = \frac{a_0}{2}(\psi - \psi_0)^2 + \frac{3}{2}A_0, \tag{5.7.9}$$

$$\check{\rho}(\mathcal{R}, \Theta) = \begin{cases} 1, & \mathcal{R} > \mathcal{C}_2 \\ 2, & \mathcal{R} < \mathcal{C}_2 \end{cases}, \tag{5.7.10}$$

and

$$\mathcal{C}_1(\Theta) = \frac{a_0}{2}(\psi - \psi_0)^2 + \frac{A_0}{2}\left(3 - \frac{1}{\pi}\arctan\sqrt{-\psi}\right), \tag{5.7.11}$$

$$\check{\rho}(\mathcal{R},\Theta)=\begin{cases}1, & \mathcal{R}>\mathcal{C}_1\\ 2-\frac{1}{\pi}\arctan\sqrt{-\psi}, & \mathcal{R}<\mathcal{C}_1\end{cases}, \tag{5.7.12}$$

respectively. Here $\psi_0$ is a constant of integration.

In the neighborhood of point B, the solution will be smooth, and the governing equation is obtained by eliminating $\check{v}$ from the system of equation (5.7.3) and is given by

$$(A_0\check{\rho}-\mathcal{R})\check{\rho}_{\mathcal{R}\mathcal{R}}-A_0\check{\rho}_{\mathcal{R}}^2-(1/2)\check{\rho}_{\mathcal{R}}+(a_0/2)\check{\rho}_{\Theta\Theta}=0. \tag{5.7.13}$$

Observe that, equation (5.7.13) exhibits distinct behaviour depending on the relationship between $A_0\check{\rho}$ and $\mathcal{R}$. Specifically, when $A_0\check{\rho}>\mathcal{R}$, the equation is elliptic, while it becomes hyperbolic for $A_0\check{\rho}<\mathcal{R}$. At the critical condition $A_0\check{\rho}=\mathcal{R}$, two sonic lines emerge: $\mathcal{S}^1$ defined by $\mathcal{R}=A_0$ and $\mathcal{S}^2$ defined by $\mathcal{R}=2A_0$.

Moreover, equation (5.7.9) describes a parabolic curve in the $(\mathcal{R},\psi)$ - plane. In contrast, equation (5.7.11) may show transition from a parabolic shape to a straight line as $\psi$ (with $\psi<0$) decreases. However, for sufficiently large negative values of $\psi$, where $\arctan\sqrt{-\psi}$ approaches $\pm\pi/2$, the second term in equation (5.7.11) converges to either $5/(2A_0)$ or $7/(2A_0)$, thereby recovering a parabolic form.

## 5.8 Numerical Results and Discussion

Diffracted shock, expansion wave profiles, as well as the shock position, are explained in this section for various values of the considered parameters. In Section 5.8.1, the behaviour of diffracted shock and expansion wave profiles is plotted. Further, the shock speed is discussed in Section 5.8.2.

### 5.8.1 Diffraction and Expansion wave Profile

In this section, the shock wave solutions are illustrated in the $(\tilde{\rho}, \omega)$-plane. The shock wave profile defined by equation (5.5.8) is plotted using equation (5.5.17) and (5.5.12), as shown in Fig. 5.2. The parameters used are $n = 1.4$, $B' = 0.5$, $\alpha = 0.5$, and $\eta = 5\pi/6$.

The solid line $h_1 s_1 \cup g_1 h_3$ represents the shock wave profile for $b' = 0$, with the dashed segment $s_1 g_1$ indicating the jump in the profile and $g_1$ marking the shock position. Similarly, for $b' = 0.3$, and $b' = 0.4$, the solid lines $h_2 s_2 \cup g_2 h_3$ and $h_2 s_3 \cup g_3 h_3$ show the shock wave profile, while the dashed segments $s_2 g_2$ and $s_3 g_3$ denote the jumps and $g_2$, and $g_3$ identify the shock positions, respectively.

It is evident that for $\omega < \omega_s = g_i; g_i = 1, 2, 3$, the solution $\tilde{\rho}$ follows the upper half of the parabola; at $\omega = \omega_s$, the shock is located; and for $\omega > \omega_s$, the boundary condition $\tilde{\rho} = \rho_i^{(2)}$ is satisfied. Notably, varying $b'$ alters both the shock position

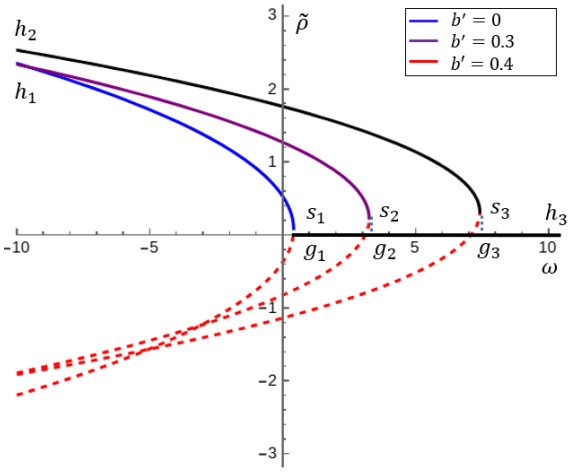


FIGURE 5.2: Plots of diffracted shock wave profile equation (5.5.8) with $n = 1.4, B' = 0.5, \alpha = 0.5, \eta = 5\pi/6$, $\rho_2^{(j)} = 0$. Solid lines $h_1 s_1 \cup g_1 h_3$, $h_1 s_2 \cup g_2 h_3$ and $h_2 s_3 \cup g_3 h_3$ represent shock wave profiles for $b' = 0, 0.3$ and $b' = 0.4$, respectively. Segments $s_1 g_1$, $s_2 g_2$, and $s_3 g_3$ are jumps in shock profiles corresponding to $b' = 0, 0.3$ and $b' = 0.4$, respectively. Here, $g_1, g_3$ and $g_3$ represent shock positions for $b' = 0, 0.3$ and $b' = 0.4$, respectively.

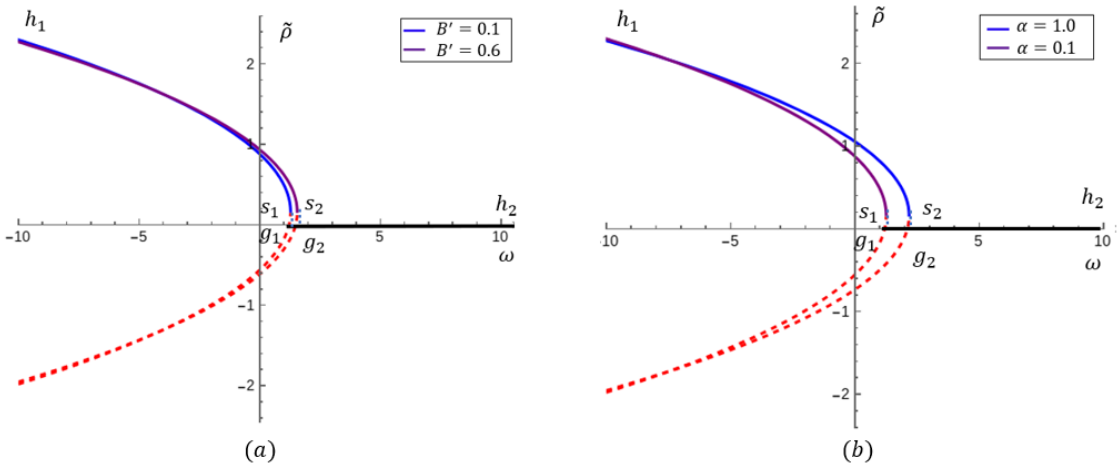


FIGURE 5.3: Plots of diffracted shock wave profile equation (5.5.8) with (a) $n = 1.4, b' = 0.2, \alpha = 0.5, \eta = 5\pi/6$, $\rho_2^{(j)} = 0$, (b) $n = 1.4, b' = 0.2, B' = 0.6, \eta = 5\pi/6$, $\rho_2^{(j)} = 0$. $s_1g_1$ and $s_2g_2$ are jumps in shock profiles for $B' = 0.1$ and 0.6, respectively. Here, $g_1$ and $g_2$ are shock positions corresponding to $B' = 0.1$ and 0.6, respectively.

and the magnitude of the jump in $\tilde{\rho}$, which reflects a change in the shock's strength. Therefore, with an increase in the values of $b'$, the boundary AB becomes stronger in extended Chaplygin gas than in the ideal gas.

In Figs. 5.3(a) and 5.3(b), the shock wave solutions are displayed for two sets of

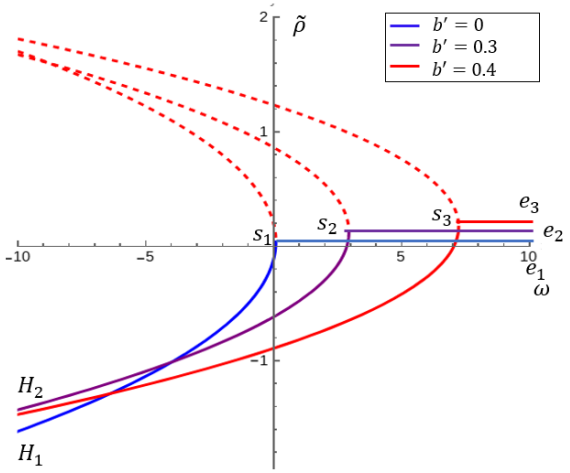


FIGURE 5.4: Plots of expansion wave profile, $\tilde{\rho}$ vs. $\omega$: equation (5.5.8) with $n = 1.4, B' = 0.5, \alpha = 0.5, \eta = 4\pi/3$. Solid lines $H_1s_1e_1$, $H_2s_2e_2$ and $H_2s_3e_3$ represent expansion wave profiles for $b' = 0, 0.3$ and $b' = 0.4$, respectively.

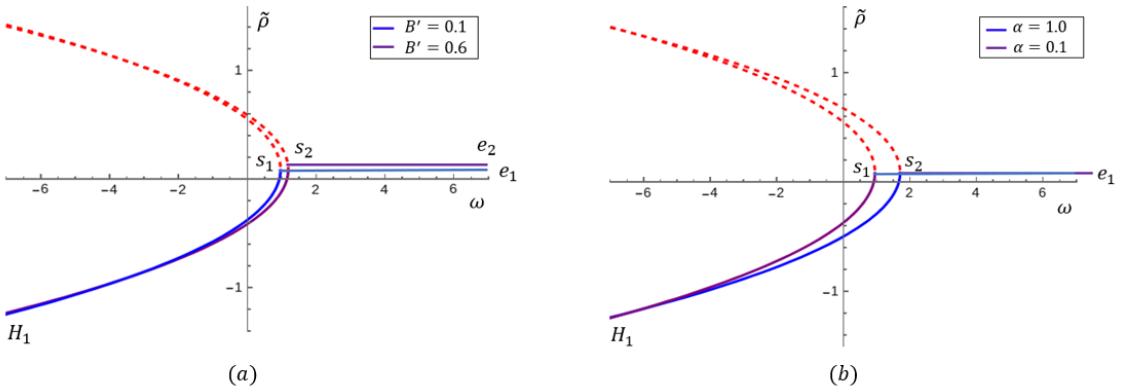


FIGURE 5.5: Plots of expansion wave profile, $\tilde{\rho}$ vs. $\omega$: equation (5.5.8) with (a) $n = 1.4, b' = 0.2, \alpha = 0.5, \eta = 4\pi/3$ (b) $n = 1.4, b' = 0.2, B' = 0.6, \eta = 4\pi/3$.

parameters: Fig. 5.3(a) shows the results for $B' = 0.1$ and $B' = 0.6$, while Fig. 5.3(b) presents the solutions for $\alpha = 0.1$ and $\alpha = 1.0$. Notably, although the shock positions vary with different values of $B'$ and $\alpha$, the magnitude of the jump in $\tilde{\rho}$ (i.e., the shock strength) seems to be less effective.

Figs. 5.4 and 5.5 illustrate the expansion wave profiles in the self-similar plane, emphasizing the effects of the parameters $b'$, $B'$, and $\alpha$. These profiles correspond to the lower branch of the parabola defined in equation (5.5.8).

In Fig. 5.4, the plot of $\tilde{\rho}$ vs. $\omega$ is presented for the parameter set $n = 1.4$, $B' = 0.5$, $\alpha = 0.5$, $\eta = 4\pi/3$, and $\rho_2^{(j)} = 0$ while varying $b'$. The solid lines labeled $H_1 s_1 e_1$, $H_2 s_2 e_2$, and $H_2 s_3 e_3$ represent the expansion wave profiles for $b' = 0$, 0.3, and 0.4, respectively.

Similarly, in Fig. 5.5(a), the profiles $H_1 s_1 e_1$ and $H_1 s_2 e_2$ correspond to $B' = 0.1$ and $B' = 0.6$, respectively. In Fig. 5.5(b), the expansion wave profiles $H_1 s_1 e_1$ and $H_1 s_2 e_1$ are shown for $\alpha = 1.0$ and $\alpha = 0.1$, respectively.

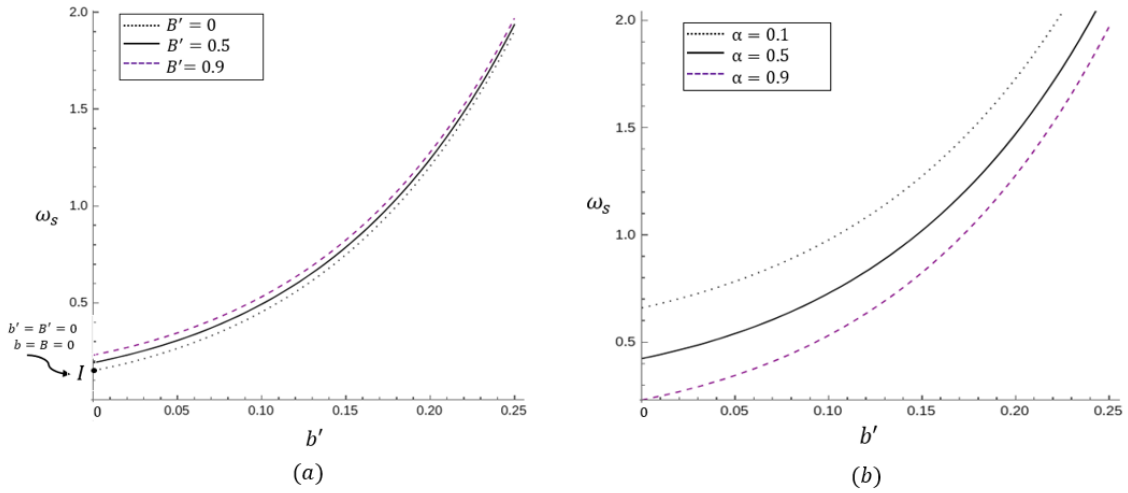


FIGURE 5.6: Plots of speed of diffracted shock $\omega_s$ vs. $b'$: equation (6.5.3) with parameters (a) $n = 1.4, \alpha = 0.1, \eta = 5\pi/6$ (b) $n = 1.4, B' = 0.9, \eta = 5\pi/6$.

### 5.8.2 Shock Position or speed of the diffracted shock

In this section, we illustrate the shock location within the self-similar plane. The position of the diffracted shock, denoted by $\omega_s$, is defined by equation (6.5.3), where $\omega_s$ represents the shock velocity in polar coordinates. The relationship between the shock location (or velocity) and the parameter $b'$ is examined for various values of $B'$ and $\alpha$ in Fig. 5.6.

Figs. 5.6(a) and 5.6(b) display the variation of $\omega_s$ with $b'$ for $B' = 0$, 0.5, 0.9 and $\alpha = 0.1$, 0.5, 0.9, respectively. In Fig. 5.6(a), the point $I$ represents the speed of the shock in an ideal gas, i.e., $b' = B' = 0$, and hence $b = \mathcal{B} = 0$. It may be observed that the shock speed in an ideal gas is slower than that in a non-ideal gas. Moreover, increasing the non-linearity parameter $B'$ results in a higher shock velocity. On the contrary, Fig. 5.6(b) shows that the shock speed decreases as the value of $\alpha$ increases.

## 5.9 Conclusions

The main objective of the present work is to unfold the impact of extended Chaplygin gas on the flow configuration on various boundaries of the whole region when a weak shock reflects and diffracts off a right-angled wedge. The flow regions are derived in the self-similar plane. Further, using R-H conditions, the asymptotic expansions of the immediate state behind the incident and reflected shock are obtained based on the given information about the state ahead of the incident shock. Next, asymptotic expansions of the flow are found in the diffracted region by solving the Laplace equation. The non-linear approximations are found to analyze the effect of singularity on diffraction-reflection phenomena. In addition, two different cases, (i) when a weak shock is coming off a wedge and (ii) when a weak shock hits the screen, are discussed, followed by the nonlinear asymptotic expansion at the intersection B of diffracted shock, reflected shock, and expansion wave profiles boundaries. With the aid of finding the asymptotic expansions in various regions and boundaries, the effect of the nonideal gas parameters $b$ and $\mathcal{B}$, and $\alpha$ is discussed for the shock and expansion wave profiles as well as for the shock speeds or shock positions. The graphical presentations of the considered parameter effects are shown. The most important highlights of the present study are summarized below:

- From the graphical illustrations, it is quite evident that the nonideal parameter $b$ alters both the shock position and the shock's strength, and both increase with the increase in $b$. Therefore, with an increase in the values of $b$, the boundary AB becomes stronger in the extended Chaplygin gas than in the ideal gas.

- The shock positions vary with different values of $\mathcal{B}$ and $\alpha$; the shock's strength seems to be less effective.

- Increase in the non-linearity parameter $\mathcal{B}$ results in a higher shock velocity. On the contrary, the shock speed decreases as the value of $\alpha$ increases.

- The rarefaction wave (expansion wave) is weakened while the diffracted shock is simultaneously strengthened by the extended Chaplygin gas effects.

***